2024 European Control Conference (ECC)
June 25-28, 2024. Stockholm, Sweden

Exploring the Impact of Memory on Network Controllability

Marco Peruzzo, Giacomo Baggio, Francesco Ticozzi

Abstract— **In this paper, we examine how adding memory to nodes of a network system impacts its controllability properties. Specifically, we analyze the behavior of the control energy of a continuous-time linear network system and that of its lifted version, obtained by allowing each node to have nontrivial internal dynamics. We discuss how to compare the effect of a control input on the original and lifted network, and show that, for line networks, adding memory may reduce the worst-case control energy by a factor that is exponential in the network size.**

I. Introduction

In the last decade the research in control theory has focused on the analysis of increasingly interconnected systems of possibly heterogeneous components. This interest is motivated by the wide range of applications which can be framed in the context of networks, such as power networks [1], social networks [2], robotic networks [3] and traffic flow networks [4]. Exploiting the capabilities of all different units composing these systems to achieve a common objective holds great potential. However, controlling large-scale network systems may easily become difficult and expensive [5]. In fact, for many complex networks the system parameters are not precisely known, the connections between different units are several and intricate, and the energy necessary to control them scales exponentially with their size [6], [7].

Among all the possible aspects related to the control of complex networks, in this work we focus on the reduction of the control effort. We do so by borrowing an idea used in the Markov chain context to obtain faster spreading of the process distribution on the underlying graph: a directional evolution can be induced by introducing suitable memory effects [8]–[10]. In our case, the memory is added by introducing local internal dynamics in the network nodes, effectively lifting the evolution to an expanded graph. We show that, when suitably tuning the internal dynamics parameters, the network with extra memory can outperform the original one in terms of control energy performance.

Contribution. The contribution of this paper is threefold. First, we extend the idea of graph lift, initially proposed for Markov chains, to continuous-time linear network systems with inputs, and introduce constraints that ensure a comparable impact of inputs on both the lifted and original networks. Next, we apply the lifting operation to line networks and establish an analytical condition guaranteeing that the worst-case control energy in the lifted network grows exponentially slower than in the original network as their sizes increase. Lastly, we complement our theoretical results with a set of numerical experiments, offering further insights into the conditions under which the lifted network exhibits a control energy advantage over its original counterpart.

Organization. The paper is organized as follows. Section II contains some background on energy-related controllability of linear network systems and presents the control energy metrics employed in our analysis. Section III introduces the notion of graph lift and illustrates how to apply it to networks with inputs. Section IV examines the worst-case control energy behavior of lifted line networks and provides a condition that guarantees an improvement in the control energy performance for the lifted network. Section V expands upon the findings from the previous section through the use of numerical simulations. Section VI concludes the paper with some remarks and future research directions.

Notation. We let $\mathrm{Re}(z)$ and $|z|$ be the real part and the absolute value of a complex number $z \in \mathbb{C}$. We denote with $\mathbb{R}^{n\times m}$ the set of $n \times m$ matrices with real entries. We let $[v]_i$ denote the i-th entry of vector $v \in \mathbb{R}^n$, and $A^\top$, $[A]_{ij}$ denote the transpose, (i,j)-th entry, respectively, of matrix $A \in \mathbb{R}^{n\times m}$. The symbols I_n, 0_n, $e_{i,n}$ stand for the identity matrix, the n-dimensional vector of zeros, and the i-th canonical vector of $\mathbb{R}^n$, respectively. We will drop the subscript n when the dimension is clear from the context. We denote with $\|A\|$ the 2-norm of matrix A. For a square matrix $A \in \mathbb{R}^{n\times n}$, $\det(A), \mathrm{trace}(A)$ and $\lambda(A)$ stand for the determinant, trace and set of eigenvalues (or spectrum) of A, respectively. A matrix A is Hurwitz if $\mathrm{Re}(\lambda) < 0$, $\forall\, \lambda \in \lambda(A)$. For a symmetric matrix $A \in \mathbb{R}^{n\times n}$ we let $\lambda_{\min}(A) := \min\{\lambda : \lambda \in \lambda(A)\}$ and $\lambda_{\max}(A) := \max\{\lambda : \lambda \in \lambda(A)\}$. We label with $\mathbf{1}_{\mathcal{C}}(\cdot)$ the indicator function of a subset $\mathcal{C} \subseteq \mathbb{R}$. Finally, we let $\mathrm{diag}\{a_1, \ldots, a_n\}$ indicate the diagonal matrix with diagonal entries a_1, …, $a_n \in \mathbb{R}$.

II. Preliminaries on energy-related network controllability

We consider a network described by a directed graph $\mathcal{G} = (\mathcal{V}, \mathcal{E})$ where $\mathcal{V} = \{1, ..., n\}$ is the set of nodes and $\mathcal{E} \subseteq \mathcal{V} \times \mathcal{V}$ is the set of edges. The state of the network at time $t \in \mathbb{R}$ is described by the vector $x(t) = \big[x_1(t), \ldots, x_n(t)\big]^\top$, whose entry $x_i(t) \in \mathbb{R}$ is the state of node $i \in \mathcal{V}$. We label with $\mathcal{K} := \{k_1, \ldots, k_m\} \subseteq \mathcal{V}$ the set of control nodes, i.e., the set of nodes within the network where a vector of independent external control signals $u(t) = [u_1(t), \ldots, u_m(t)]^\top$ enter the network.

We assume that the evolution of the state $x(t)$ of the network is described by the following continuous-time linear and time invariant dynamics

$$\dot{x}(t) = Ax(t) + Bu(t), \tag{1}$$

where $A \in \mathbb{R}^{n\times n}$ is the adjacency (or network) matrix of $\mathcal{G}$, that is, the entry $[A]_{ij}$ is the weight associated to the edge

$(j,i) \in \mathcal{E}$ and $[A]_{ij} = 0$ if $(j,i) \notin \mathcal{E}$, and $B \in \mathbb{R}^{n\times m}$ is made of a subset of canonical vectors of $\mathbb{R}^n$, namely,

$$B = [e_{k_1}, \dots, e_{k_m}], \quad \{k_1, \dots, k_m\} \in \mathcal{K}. \tag{2}$$

The network system (1) is said to be controllable if for any final state $x_\mathrm{f} \in \mathbb{R}^n$ there exists an external input able to steer the system state from $x(0) = 0$ to $x(T) = x_\mathrm{f}$ within a certain, possibly infinite, time horizon $[0, T]$. Controllability can be checked using Kalman's rank condition [11] which makes use of the controllability matrix, defined as

$$\mathcal{C}_T = \begin{bmatrix} B & AB & \cdots & A^{T-1}B \end{bmatrix}. \tag{3}$$

The system is controllable in $[0, T]$ if and only if the controllability matrix (3) has full row rank. The concept of controllability is qualitative and does not provide a measure of the specific control effort necessary to reach a desired state configuration. Whenever we want to quantitatively characterize controllability of a network system, we can rely on the controllability Gramian of (1), defined as

$$\mathcal{W}_T = \int_0^T e^{At} B B^\top e^{A^\top t} \mathrm{d}t. \tag{4}$$

The Gramian $\mathcal{W}_T$ is a positive definite matrix for $T > 0$ if and only if the system is controllable in $[0, T]$. Moreover, for $T \to \infty$, the Gramian is well defined if and only if the matrix A in (1) is Hurwitz. If we assume the system (1) to be controllable, the minimum energy control input steering the system from $x(0) = 0$ to $x(T) = x_\mathrm{f}$ is given by [11]

$$u^*(t) = B^\top e^{A^\top (T-t)} \mathcal{W}_T^{-1} x_\mathrm{f}, \quad t \in [0, T], \tag{5}$$

and the energy of this optimal input is

$$\mathrm{E}(u^*(t)) = \int_0^T \|u^*(t)\|^2 \mathrm{d}t = x_\mathrm{f}^\top \mathcal{W}_T^{-1} x_\mathrm{f}. \tag{6}$$

Equation (6) highlights how the (minimum) energy required to control the network system (1) is related to the inverse of the Gramian $\mathcal{W}_T$. As a consequence, it is possible to employ scalar functions of the eigenvalues of $\mathcal{W}_T$ to define quantitative controllability metrics. Different metrics have been proposed over the years, including $\lambda_{\min}(\mathcal{W}_T)$, $\mathrm{trace}(\mathcal{W}_T^{-1})$, $\det(\mathcal{W}_T)$, $\lambda_{\max}(\mathcal{W}_T)$ [7], [12].

In the remaining of this paper, we restrict the analysis to Hurwitz stable systems and infinite horizon ($T \to \infty$) controllability Gramians, which we denote simply by $\mathcal{W}$. Further, we focus on the metric $\lambda_{\min}(\mathcal{W})$, whose inverse is equal to the worst-case control energy to reach a unit-norm target state x_f. Notably, it has been shown that for networks with symmetric (or almost symmetric) adjacency matrices controlled by a limited number of nodes, $\lambda_{\min}(\mathcal{W})$ decays exponentially in the network size n, which implies that the worst-case control energy $1/\lambda_{\min}(\mathcal{W})$ grows exponentially in n [6], [7]. In this situation, the degree of controllability of networks can be quantified via the asymptotic exponential rate of the worst-case control energy, namely,[1]

$$\rho = \lim_{n\to\infty} \frac{1}{n} \ln\left(\frac{1}{\lambda_{\min}(\mathcal{W})}\right). \tag{7}$$

This metric has been introduced in [13] under the name of *worst-case control energy exponent*.

Finally, when the natural quantity of interest for control is an output of the system

$$y(t) = Cx(t), \quad C \in \mathbb{R}^{p\times n},$$

rather than its state, we can introduce the output controllability Gramian which is defined as $\mathcal{W}_o = C\mathcal{W}C^\top$, where $\mathcal{W}$ is the (infinite-horizon) controllability Gramian introduced in (4). It is possible to quantify the output control energy (i.e., the energy required to control the system output) and its asymptotic exponential rate by evaluating the same metrics defined before on $\mathcal{W}_o$ rather than on $\mathcal{W}$.

III. Lifting networks with inputs

In this section, we discuss how it is possible to endow each of the nodes in the network system (1) with a local memory on the direction of the received control inputs from neighboring nodes or from the external environment. We will later exploit this extra memory to improve the controllability performance of the network.

The way we endow nodes with additional memory is by enlarging the dimension of the state space of the nodes. Specifically, we associate to $\mathcal{G}$ a new graph $\hat{\mathcal{G}}$ called lifted graph, which is defined as follows.

Definition 1: ***(Lift of a graph)*** A graph $\hat{\mathcal{G}} = (\hat{\mathcal{V}}, \hat{\mathcal{E}})$ on $\hat{n}$ nodes is called a lift of $\mathcal{G}$ if there exist a surjective map $\zeta\colon \hat{\mathcal{V}} \to \mathcal{V}$ such that

$$(i,j) \in \hat{\mathcal{E}} \implies (\zeta(i), \zeta(j)) \in \mathcal{E}.$$

Further, we denote with ζ^{-1} the map which takes as input a node $k \in \mathcal{V}$ and outputs all nodes $j \in \hat{\mathcal{V}}$ for which $\zeta(j) = k$.

The lift is said to be *regular* if for each node of the original graph $\mathcal{G}$ the lifted graph $\hat{\mathcal{G}}$ contains the same fixed number K of associated nodes. More formally, in a regularly lifted graph the cardinality of the set $\hat{\mathcal{V}}_j = \zeta^{-1}(j)$ is equal to K for all $j \in \mathcal{V}$. We may hence think of the regularly lifted network as a network composed by n subgraphs of K nodes $\hat{\mathcal{G}}_i = (\hat{\mathcal{V}}_i, \hat{\mathcal{E}}_i), i \in \mathcal{V}$, where $\hat{\mathcal{V}}_i = \{1, \dots, K\}$ and $\hat{\mathcal{E}}_i \subseteq \hat{\mathcal{V}}_i \times \hat{\mathcal{V}}_i$. Moreover, if the interconnections between the K nodes in the same subgraph are identical, the lift is called *homogeneous*. In this paper, we restrict the attention only to regular homogeneous lifts.

By performing a lift we are introducing a new network system different from the original one, whose topology is characterized by the graph $\hat{\mathcal{G}} = (\hat{\mathcal{V}}, \hat{\mathcal{E}})$. The state of the lifted network at time $t \in \mathbb{R}$ is described by the vector $\hat{x}(t) \in \mathbb{R}^{nK}$, where K is the number of nodes in $\hat{\mathcal{V}}_i$, $i \in \mathcal{V}$, whereas $\hat{u}(t) \in \mathbb{R}^{\hat{m}}$ denotes the vector of external inputs. The evolution of

[1] In what follows, when taking the limit for $n \to \infty$, we implicitly assume the existence of a sequence of systems as in (1), with state matrices and input matrices of increasing dimension n.

the state $\hat{x}(t)$ is governed by the following continuous-time linear and time invariant dynamics:

$$\dot{\hat{x}}(t) = \hat{A}\hat{x}(t) + \hat{B}\hat{u}(t), \tag{8}$$

where $\hat{A} \in \mathbb{R}^{nK\times nK}$ is the adjacency matrix of $\hat{\mathcal{G}}$ and $\hat{B} \in \mathbb{R}^{nK\times\hat{m}}$ is an input matrix. The lifted system (8) is the interconnection of n subsystems, each describing the dynamics running on subgraph $\hat{\mathcal{G}}_i$, $i = 1,\dots,n$. The state $\hat{x}_i(t)$ of the i-th subsystem obeys the dynamics

$$\dot{\hat{x}}_i(t) = \hat{A}_i\hat{x}_i(t) + \sum_{j\neq i}\hat{A}_{i,j}\hat{x}_j(t) + \hat{B}_i\hat{u}(t), \tag{9}$$

where $\hat{A}_i \in \mathbb{R}^{K\times K}$ is the adjacency matrix of $\hat{\mathcal{G}}_i$, $\hat{A}_{i,j} \in \mathbb{R}^{K\times K}$ are matrices encoding the interconnections between subsystems, and $\hat{B}_i \in \mathbb{R}^{K\times\hat{m}}$ is an external input matrix.

To maintain a relation with the original network we need to impose some *topological constraints* on the lifted network system. In particular, we assume that:

A.1) If $(i,j) \in \mathcal{E}$ then there exist $h \in \zeta^{-1}(i)$, $k \in \zeta^{-1}(j)$ such that $(h,k) \in \hat{\mathcal{E}}$.

A.2) The lifted network has the same number of inputs of the original network, that is, $\hat{m} = m$.

A.3) The i-th subsystem (9) receives an external input ($\hat{B}_i \neq 0$) if and only if the i-th node of the original network is fed with an external input.

Depending on the choice of the internal dynamics in (9) of the subsystems, the collective behavior of the lifted network can significantly differ from that of the original network. Hence, whenever we want to compare the controllability properties of the two networks, it is necessary to understand under which conditions such comparison is meaningful.

It is known that proximity to instability positively influences the amplification of input signals and, consequently, controllability [14]. In light of such interplay, we impose the following *stability constraint* on the lifted subsystems:

A.4) $\max_{\lambda\in\lambda(\hat{A}_i)}\mathrm{Re}(\lambda) \leq [A]_{ii}$, $i = 1,\dots,n$.

Condition A.4 ensures that the i-th subsystem in (9) is not closer to instability than node i of the original network. This implies that the impact of stability on the controllability of the i-th subsystem is, at most, equivalent to that of node i.

Finally, to compare the state of the lifted and original network systems, we introduce the notion of state induced by the lift. This state is defined as

$$x_I(t) = \hat{C}\hat{x}(t), \tag{10}$$

where $\hat{C} \in \mathbb{R}^{n\times nK}$ will be referred to as the lift output matrix. The vector $x_I(t)$, which can be thought as an output for the lifted dynamics, has a number of entries equal to the number of nodes of the original network and represents the state of the original network after the internal dynamics of the nodes has been lifted. In particular, let $\hat{x}_{i,j}(t)$ be the j-th component of $\hat{x}_i(t)$, we will assume that the i-th component of the induced state consists of the sum of the states of the i-th subsystem in (9), that is:

A.5) $[x_I(t)]_i = \sum_j \hat{x}_{i,j}(t)$, $i = 1,\dots,n$.

In what follows, we compare, under assumptions A.1–A.5, the worst-case control energy exponents of the original network and the lifted network with output matrix as in (10).

IV. Control energy of lifted line networks

In this section we show how the lift operation introduced in the previous section can be applied to a simple yet insightful network topology. For this topology, we analytically show that, by lifting the network, the energy required to control it can be reduced by an exponential factor in the network size.

Our case study will be the symmetric bidirectional line network of n nodes with a single input applied to the first node, as depicted in Figure 1. The network system is governed by the linear time invariant dynamics in (1), with state and input matrices defined as

$$A = \begin{bmatrix} -\delta & \alpha & 0 & \dots & 0 \\ \alpha & -\delta & \alpha & \dots & 0 \\ \vdots & \alpha & \ddots & \ddots & \vdots \\ 0 & 0 & \ddots & \ddots & \alpha \\ 0 & 0 & 0 & \alpha & -\delta \end{bmatrix}, \quad B = \begin{bmatrix} \beta \\ 0 \\ 0 \\ \vdots \\ 0 \end{bmatrix}, \tag{11}$$

where α, β, δ are positive real parameters and $n \geq 2$. For large n the eigenvalues of A take values in the interval $\Lambda := [-\delta-2\alpha, -\delta+2\alpha]$ with density (see e.g. [13]):

$$p(\lambda) = \frac{1}{\pi\sqrt{4\alpha^2-(\lambda+\delta)^2}}\mathbf{1}_\Lambda(\lambda). \tag{12}$$

Finally, we impose A to be Hurwitz by setting $\delta > 2\alpha$.

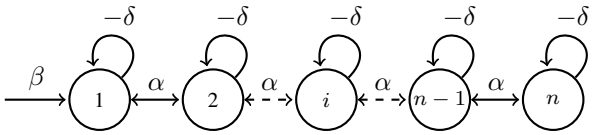

Fig. 1. The symmetric bidirectional line network considered in this work. The input enters from node 1 with weight $\beta > 0$, the parameter $\alpha > 0$ is the edge weight and $-\delta < 0$ is the self-loop weight.

The following lemma characterizes the worst-case control energy exponent (7) of the above network.

Lemma 1: ***(Worst-case control energy exponent of line networks)*** Consider the line network described in (11). The worst-case control energy exponent of the network is

$$\rho = 2\ln\left(1 + \frac{\sqrt{\delta^2+2\delta\alpha}+\delta}{\alpha}\right). \tag{13}$$

Proof: From [13, Theorem 4], the worst-case control energy exponent of the network in (11) can be computed as

$$\rho = \max_{\lambda\in\Lambda}\int_\Lambda 2\ln\left|\frac{\lambda+\mu}{\lambda-\mu}\right|p(\mu)\mathrm{d}\mu,$$

where $p(\cdot)$ is the asymptotic eigenvalue density in (12). Let

$$\begin{aligned} f(\lambda) &:= \int_\Lambda 2\ln\left|\frac{\lambda+\mu}{\lambda-\mu}\right|p(\mu)\mathrm{d}\mu \\ &= \int_\Lambda \ln(\lambda+\mu)^2 p(\mu)\mathrm{d}\mu - \int_\Lambda \ln(\lambda-\mu)^2 p(\mu)\mathrm{d}\mu. \end{aligned} \tag{14}$$

From [15, Corollary 3], the following identity holds:

$$\int_\Lambda \ln(\lambda-\mu)^2 p(\mu)\mathrm{d}\mu = \begin{cases} 2\ln\alpha & \text{if } \lambda\in\Lambda, \\ 2\ln\alpha + 2\ln\left(\left|\frac{\delta+\lambda}{2\alpha}\right| + \sqrt{\left(\frac{\delta+\lambda}{2\alpha}\right)^2-1}\right) & \text{if } \lambda\notin\Lambda. \end{cases} \tag{15}$$

Note that if $\lambda\in\Lambda$ then $-\lambda\notin\Lambda$, since A is Hurwitz. As a consequence, if $\lambda\in\Lambda$, equation (15) yields

$$\int_\Lambda \ln(\lambda+\mu)^2 p(\mu)\mathrm{d}\mu = \int_\Lambda \ln(-\lambda-\mu)^2 p(\mu)\mathrm{d}\mu$$
$$= 2\ln\alpha + 2\ln\left(\frac{\delta-\lambda}{2\alpha} + \sqrt{\left(\frac{\delta-\lambda}{2\alpha}\right)^2-1}\right).$$

Therefore, by plugging (15) into (14) and assuming $\lambda\in\Lambda$,

$$f(\lambda) = 2\ln\left(\frac{\delta-\lambda}{2\alpha} + \sqrt{\left(\frac{\delta-\lambda}{2\alpha}\right)^2-1}\right).$$

Finally, the maximum of the above function in the interval Λ is attained at $\lambda^* := -\delta-2\alpha$, which yields

$$\rho = \max_{\lambda\in\Lambda} f(\lambda) = f(\lambda^*) = 2\ln\left(1+\frac{\sqrt{\delta^2+2\delta\alpha}+\delta}{\alpha}\right),$$

and concludes the proof. ∎

We now apply the lift operation to the line network (11) by enlarging the state space of each node, as described in the previous section. Note that in the symmetric line network (11) each node (except for the first and last node) receives inputs from either its left neighbor or its right neighbor, and possibly from the external environment. To retain the information on the direction of the received control input, we associate to each node in the original network two nodes in the corresponding lifted line network. More formally, we consider the lifted graph $\hat{\mathcal{G}} = (\hat{\mathcal{V}}, \hat{\mathcal{E}})$ where $\hat{\mathcal{V}} = \{1, 2, \dots, 2n\}$, $\hat{\mathcal{E}} = \hat{\mathcal{V}}\times\hat{\mathcal{V}}$ and a map $\zeta\colon \hat{\mathcal{V}}\to\mathcal{V}$ so that $\zeta^{-1}(i) = \{i, n+i\}$. The first node of the lifted subsystem receives inputs from the left neighbor and propagates them to the right, the second node instead receives signals form the right neighbor and propagates them to the left. Furthermore, we allow for some exchange of information between the two nodes in each subsystem of the lifted network. The resulting network is depicted in Figure 2. The dynamics of the lifted network is described by (8) with system matrices set as:

$$\hat{A} = \begin{bmatrix} \hat{A}_1 & \hat{\epsilon} I_n \\ \hat{\epsilon} I_n & \hat{A}_2 \end{bmatrix}, \quad \hat{B} = \begin{bmatrix} \hat{\beta} \\ 0_{n-1} \\ \hat{\beta} \\ 0_{n-1} \end{bmatrix}, \tag{16}$$

where α, $\hat{\beta}$, $\hat{\delta}$, $\hat{\epsilon}$ are real parameters with α, $\hat{\beta}$, $\hat{\delta} > 0$ and

$$\hat{A}_1 = \begin{bmatrix} -\hat{\delta} & 0 & \cdots & 0 \\ \alpha & -\hat{\delta} & \ddots & \vdots \\ & \ddots & \ddots & 0 \\ 0 & & \alpha & -\hat{\delta} \end{bmatrix}, \quad \hat{A}_2 = \begin{bmatrix} -\hat{\delta} & \alpha & & 0 \\ 0 & \ddots & \ddots & \\ \vdots & \ddots & -\hat{\delta} & \alpha \\ 0 & \cdots & 0 & -\hat{\delta} \end{bmatrix}.$$

In designing the lift, the degrees of freedom are the self-loop weight $-\hat{\delta}$, the input weight $\hat{\beta}$, and $\hat{\epsilon}$ which is the weight associated to the (symmetric) interconnection between the two nodes within the same lifted subsystem. To preserve the topology of the original network we impose the same interconnection weight α between neighboring subsystems. Moreover, to split equally the control signal within the two nodes in the first subsystem we set $\hat{\beta} = \beta/2$.[2] Notice that the designed lift respect the topological constraints A.1, A.2, A.3 of the previous section. As for the stability constraint (condition A.4) we need to impose $-\hat{\delta}+\hat{\epsilon} \le -\delta$. Lastly, following assumption A.5, we define the lift output matrix as

$$\hat{C} = \begin{bmatrix} I_n & I_n \end{bmatrix}. \tag{17}$$

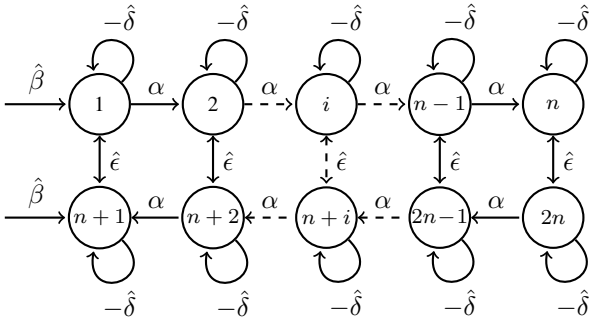

Fig. 2. The lifted line network considered in this work. The i-th subsystem of the lifted network comprises nodes i and $n+i$.

In the following lemma we establish an expression for the worst-case control energy exponent of the lifted line network with output matrix $\hat{C}$ in (17). This expression applies to the particular case of no interconnection between the nodes within each subsystem, i.e., $\hat{\epsilon} = 0$. Note that in this case the matrix $\hat{A}$ is Hurwitz for any choice of α, $\hat{\delta} > 0$. Observe also that, in this case, the lifted network is not controllable; indeed the nodes $n+2, \dots, 2n$ cannot be reached by the input. However, as shown in the proof of the lemma, the lifted network is output controllable, i.e., the induced state x_I can be steered to any desired value via suitable inputs.

Lemma 2: ***(Worst-case control energy exponent of lifted line networks for*** $\hat{\epsilon} = 0$***)*** Consider the lifted line network (16) with output matrix $\hat{C}$ as in (17) and $\hat{\epsilon} = 0$. The worst-case control energy exponent of the network is

$$\hat{\rho} = 2\ln\left(1+\frac{2\hat{\delta}}{\alpha}\right). \tag{18}$$

[2]It can be shown (see the proof of Lemma 2) that the particular choice of $\hat{\beta} > 0$ does not impact the controllability performance for large networks, as quantified by the worst-case control energy exponent.

Proof: The (output) controllability Gramian of the lifted network with $\hat{\epsilon} = 0$ can be written as

$$\begin{aligned}\mathcal{W}_o &= \int_0^\infty \hat{C}e^{\hat{A}t}\hat{B}\hat{B}^\top e^{\hat{A}^\top t}\hat{C}^\top \mathrm{d}t \\ &= \hat{\beta}^2\int_0^\infty (e^{\hat{A}_1 t}e_1 + e^{\hat{A}_2 t}e_1)(e_1^\top e^{\hat{A}_1^\top t} + e_1^\top e^{\hat{A}_2^\top t})\mathrm{d}t \\ &= \underbrace{\hat{\beta}^2\int_0^\infty e^{\hat{A}_1 t}e_1e_1^\top e^{\hat{A}_1^\top t}\mathrm{d}t}_{\mathcal{W}_1} + \underbrace{\hat{\beta}^2\int_0^\infty e^{\hat{A}_2 t}e_1e_1^\top e^{\hat{A}_2^\top t}\mathrm{d}t}_{\mathcal{W}_2} \\ &+ \underbrace{\hat{\beta}^2\int_0^\infty (e^{\hat{A}_1 t}e_1e_1^\top e^{\hat{A}_2^\top t} + e^{\hat{A}_2 t}e_1e_1^\top e^{\hat{A}_1^\top t})\mathrm{d}t}_{\mathcal{W}_3}. \end{aligned} \tag{19}$$

We next compute separately the three matrices $\mathcal{W}_1$, $\mathcal{W}_2$, $\mathcal{W}_3$. From [16, Proposition 1], it holds

$$[e^{\hat{A}_1 t}e_1]_i = e^{-\delta t}\frac{(\alpha t)^{i-1}}{(i-1)!}. \tag{20}$$

Further,

$$[e^{\hat{A}_2 t}e_1]_i = \begin{cases} e^{-\delta t} & \text{if } i = 1, \\ 0 & \text{if } i \neq 1. \end{cases} \tag{21}$$

By using (20) and (21) in (19), it follows that

$$\begin{aligned}[\mathcal{W}_o]_{ij} &= [\mathcal{W}_1 + \mathcal{W}_2 + \mathcal{W}_3]_{ij} \\ &= \begin{cases} 4[\mathcal{W}_1]_{ij} & \text{if } i = j = 1, \\ 2[\mathcal{W}_1]_{ij} & \text{if } i = 1 \text{ or } j = 1 \text{ and } i \neq j, \\ [\mathcal{W}_1]_{ij} & \text{otherwise.} \end{cases}\end{aligned}$$

The above Gramian can be written more compactly as

$$\mathcal{W}_o = D\mathcal{W}_1 D, \quad \text{with} \quad D = \mathrm{diag}\{2, 1, \dots, 1\}.$$

From the previous expression, it holds

$$\begin{aligned}\lambda_{\min}(\mathcal{W}_o) &= \min_{\substack{x\in\mathbb{R}^n \\ x\neq 0}} \frac{x^\top \mathcal{W}_o x}{x^\top x} = \min_{\substack{x\in\mathbb{R}^n \\ x\neq 0}} \frac{x^\top D\mathcal{W}_1 D x}{x^\top x} \\ &= \min_{\substack{y = Dx\in\mathbb{R}^n \\ y\neq 0}} \frac{y^\top \mathcal{W}_1 y}{y^\top D^{-\top}D^{-1}y},\end{aligned} \tag{22}$$

Moreover, it is possible to observe that

$$\begin{aligned}y^\top D^{-1}D^{-1}y &\geq \lambda_{\min}(D^{-1}D^{-1})y^\top y = y^\top y/\|D\|^2, \\ y^\top D^{-1}D^{-1}y &\leq \lambda_{\max}(D^{-1}D^{-1})y^\top y = \|D^{-1}\|^2 y^\top y.\end{aligned}$$

From (22) and the above inequalities, it follows that

$$\begin{aligned}\lambda_{\min}(\mathcal{W}_o) &\leq \|D\|^2 \min_{\substack{y\in\mathbb{R}^n \\ y\neq 0}} \frac{y^\top \mathcal{W}_1 y}{y^\top y} = \|D\|^2\lambda_{\min}(\mathcal{W}_1) \\ &= 4\lambda_{\min}(\mathcal{W}_1), \\ \lambda_{\min}(\mathcal{W}_o) &\geq \frac{1}{\|D^{-1}\|^2} \min_{\substack{y\in\mathbb{R}^n \\ y\neq 0}} \frac{y^\top \mathcal{W}_1 y}{y^\top y} = \frac{1}{\|D^{-1}\|^2}\lambda_{\min}(\mathcal{W}_1) \\ &= \lambda_{\min}(\mathcal{W}_1).\end{aligned}$$

The latter bounds readily imply that

$$\hat{\rho} = \lim_{n\to\infty}\frac{1}{n}\ln\left(\frac{1}{\lambda_{\min}(\mathcal{W}_o)}\right) = \lim_{n\to\infty}\frac{1}{n}\ln\left(\frac{1}{\lambda_{\min}(\mathcal{W}_1)}\right)$$

Finally, from the asymptotic behavior of $\lambda_{\min}(\mathcal{W}_1)$ derived in [7, Table 1], we conclude that

$$\hat{\rho} = \lim_{n\to\infty}\frac{1}{n}\ln\left(\frac{1}{\lambda_{\min}(\mathcal{W}_1)}\right) = 2\ln\left(1 + \frac{2\hat{\delta}}{\alpha}\right). \tag{23}$$

■

The following result, which builds on the previous lemmas, provides a condition under which the lifted line network outperforms the original network in terms of control energy.

Theorem 1: ***(Control energy advantage of lifted networks for*** $\hat{\epsilon} = 0$***)*** Consider the line network (11) and its lifted version (16) with output matrix $\hat{C}$ as in (17). Let ρ and $\hat{\rho}$ denote the worst-case control energy exponent of the original and lifted network, respectively. It holds

$$\rho > \hat{\rho} \iff \sqrt{\delta^2 + 2\delta\alpha} > 2\hat{\delta} - \delta. \tag{24}$$

Proof: From the expressions of ρ and $\hat{\rho}$ in Lemma 1 and 2, the inequality $\rho > \hat{\rho}$ holds if and only if

$$\begin{aligned}&2\ln\Big(1 + \frac{\sqrt{\delta^2 + 2\delta\alpha} + \delta}{\alpha}\Big) > 2\ln(1 + \frac{2\hat{\delta}}{\alpha}) \\ \iff\ &\frac{\sqrt{\delta^2 + 2\delta\alpha} + \delta}{\alpha} + 1 > 1 + \frac{2\hat{\delta}}{\alpha} \\ \iff\ &\sqrt{\delta^2 + 2\delta\alpha} + \delta > 2\hat{\delta}.\end{aligned}$$

This yields (1) and concludes the proof. ■

A few comments on the above result are in order. First, notice that, by setting $\hat{\delta} = \delta$, the condition in Theorem 1 reads as

$$\rho > \hat{\rho} \iff \sqrt{\delta^2 + 2\delta\alpha} > \delta,$$

which is always satisfied because $\alpha, \delta > 0$. In this case, we always have an advantage in employing the lifted dynamics. Second, and more importantly, we remark that the condition in Theorem 1 is in terms of control energy exponents. This means that, when this condition is satisfied, the gap between the worst-case control energy of the original network and its lifted counterpart grows exponentially with the network size.

V. Numerical analysis

In this section we present some numerical simulations which complement the theoretical analysis of the previous section. In particular, we focus on an empirical comparison between the behavior of the worst-case control energy of the line network (11) and its lifted counterpart (16).

In Figure 3, we compare the worst-case control energy exponent of the original and lifted network. Specifically, we plot the quantity

$$\Delta = \hat{\gamma} - \gamma, \tag{25}$$

as a function of network parameters $\hat{\delta}$ and $\hat{\epsilon}$ (Fig. 3, top plot) and $\hat{\delta}$ and α (Fig. 3, bottom plot), where

1) γ is an empirical worst-case control energy exponent of the line network (11), computed as

$$\gamma = \frac{\ln(1/\lambda_{\min}(\mathcal{W}^{(n_2)})) - \ln(1/\lambda_{\min}(\mathcal{W}^{(n_1)}))}{n_2 - n_1},$$

where $\mathcal{W}^{(n)}$ denotes the controllability Gramian of the line network with n nodes, and $n_2 > n_1$.

2) $\hat{\gamma}$ is an empirical worst-case control energy exponent of the lifted line network (16), computed as

$$\hat{\gamma} = \frac{\ln(1/\lambda_{\min}(\mathcal{W}_o^{(2n_2)})) - \ln(1/\lambda_{\min}(\mathcal{W}_o^{(2n_1)}))}{n_2 - n_1},$$

where $\mathcal{W}_o^{(n)}$ denotes the output controllability Gramian of the lifted line network with n nodes and $n_2 > n_1$.

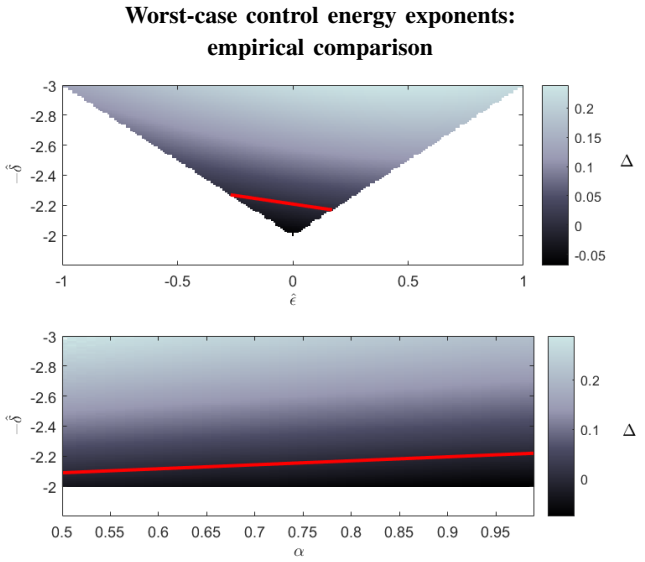

Fig. 3. Empirical comparison between the worst-case control energy exponents of the line network (11) and the lifted line network (16). We choose line network parameters $\delta = 2$, $\beta = 1$, $\hat{\beta} = 0.5$, $\alpha = 0.9$ in the top plot, and $\delta = 2$, $\beta = 1$, $\hat{\beta} = 0.5$, $\hat{\epsilon} = 0$ in the bottom plot. The plots show the values of the empirical metric Δ, as defined in (25), computed for $n_1 = 5$ and $n_2 = 8$. The white area highlights the set of parameters that do not satisfy the constraint A.4 defined in Sec. III. The red line indicates the values of parameters yielding $\Delta = 0$.

Observe that a negative value of Δ in (25) indicates that the lifted network exhibits a worst-case control energy lower than the one of the original network. Further, the white area in the plots denotes the region of parameters for which the stability constraint in A.4 is not satisfied.

It is interesting to notice that the lifted network does not outperform the original one for all choices of network parameters. In particular, when the lifted network exhibits a high degree of stability (corresponding to a large value of $\hat{\delta}$) we have $\Delta > 0$ meaning that the original network requires less energy to be controlled compared to the lifted one. On the other hand, the choice of parameters offering the greatest advantage in control energy for the lifted network is $\hat{\delta} = \delta$ and $\hat{\epsilon} = 0$. This is, as expected, a particular case of the configuration that has been shown to exhibit advantages for the lifted dynamics in Section IV, and corresponds to two decoupled, fully directed dynamics. Finally, it is worth to mention that Δ slightly increases whenever we lower the value of the parameter α, showing less advantage in employing memory to improve control energy performance for networks featuring weak interconnections.

VI. Conclusions

This paper represents an initial exploration of the role of memory effects in the control of network systems. Our study demonstrates how these effects can be effectively designed to reduce the effort needed to control a network. Specifically, our analytic and numerical findings reveal that, for line network topologies, adding local memory and exploiting it to induce directionality in the evolution can provide an advantage in control energy. Interestingly, such advantage grows exponentially with the cardinality of the network.

A number of issues still remain open for further investigation. For instance, constraints alternative to A.4 that more effectively encapsulate a desired non-amplifying behavior of the lifted subsystems can be explored. In addition, analytical expressions of control energy exponents could be derived for more general choices of line network parameters. This would provide a more precise quantification of the control benefits of the proposed strategy. Additional future work directions include the description of lifted dynamics for networks with multi-dimensional node states and the analysis of the interplay between memory and control energy in more complex network topologies.

References

[1] G. A. Pagani and M. Aiello, "The power grid as a complex network: a survey," *Physica A: Statistical Mechanics and its Applications*, vol. 392, no. 11, pp. 2688–2700, 2013.

[2] D. Acemoglu, G. Como, F. Fagnani, and A. Ozdaglar, "Opinion fluctuations and disagreement in social network," *Mathematics of Operations Research*, vol. 38, 09 2010.

[3] K. D. Listmann, M. V. Masalawala, and J. Adamy, "Consensus for formation control of nonholonomic mobile robots," in *IEEE International Conference on Robotics and Automation*, 2009, pp. 3886–3891.

[4] G. Como, "On resilient control of dynamical flow networks," *Annual Reviews in Control*, vol. 43, pp. 80–90, 2017.

[5] Y.-Y. Liu and A.-L. Barabasi, "Control principles of complex networks," *Rev. Mod. Phys.*, vol. 88, 08 2015.

[6] F. Pasqualetti, S. Zampieri, and F. Bullo, "Controllability metrics, limitations and algorithms for complex networks," *IEEE Transactions on Control of Network Systems*, vol. 1, pp. 40–52, 06 2014.

[7] G. Baggio, F. Pasqualetti, and S. Zampieri, "Energy-aware controllability of complex networks," *Annual Review of Control, Robotics, and Autonomous Systems*, vol. 5, no. 1, pp. 465–489, 2022.

[8] P. Diaconis, S. P. Holmes, and R. M. Neal, "Analysis of a nonreversible markov chain sampler," *Annals of Applied Probability*, vol. 10, pp. 726–752, 2000.

[9] S. Apers, A. Sarlette, and F. Ticozzi, "When does memory speed-up mixing?" in *2017 IEEE 56th Annual Conference on Decision and Control (CDC)*, 2017, pp. 4940–4945.

[10] ——, "Simulation of quantum walks and fast mixing with classical processes," *Physical Review A*, vol. 98, no. 3, p. 032115, 2018.

[11] R. E. Kalman, Y. Ho, and K. S. Narendra, "Controllability of linear dynamical systems," *Contributions to Differential Equations*, vol. 1, pp. 189–213, 1963.

[12] T. H. Summers, F. L. Cortesi, and J. Lygeros, "On submodularity and controllability in complex dynamical networks," *IEEE Transactions on Control of Network Systems*, vol. 3, no. 1, pp. 91–101, 2015.

[13] G. Baggio and S. Zampieri, "Controllability of large-scale networks: The control energy exponents," *IEEE Transactions on Control of Network Systems (to appear)*, 2023.

[14] F. Pasqualetti, S. Zhao, C. Favaretto, and S. Zampieri, "Fragility limits performance in complex networks," *Scientific Reports*, vol. 10, no. 1, p. 1774, 2020.

[15] K. M. Schmidt and A. Zhigljavsky, "A characterization of the arcsine distribution," *Statistics & Probability Letters*, vol. 79, pp. 2451–2455, 12 2009.

[16] S. Zhao and F. Pasqualetti, "Controllability degree of directed line networks: Nodal energy and asymptotic bounds," in *2018 European Control Conference*, 2018, pp. 1857–1862.